Supplementary figures and tables

Sulfate radicals enable a non-enzymatic Krebs cycle precursor

Markus A. Keller, Domen Kampjut, Stuart A. Harrison and Markus Ralser.

Supplementary Table 1. Reaction rate data for controls, Fe(II), peroxydisulfate and peroxydisulfate / ferrous sulfide: *“Suppl Table 1.csv”*

Supplementary Table 2. Metal dependency rate data: *“Suppl Table 2.csv”*

Supplementary Table 3. Z-score data: *“Suppl Table 3.csv”*

Supplementary Table 4. Complete reaction list: *“Suppl Table 4.csv”*

Supplementary Table 5. Scavenger experiment reaction rate data: *“Suppl Table 5.csv”*

Supplementary Table 6: Potential TCA intermediates interconversion rationale

Reaction	***Substrate***	***Product***	***Potential reaction rationale***
aco -> mal	Aconitate	Malate	A slow interconversion that is observable in the peroxydisulfate conditions only and likely is achieved via a multistep reaction path, potentially also by reduction of an initially formed succinate or succinic semialdehyde.
aco -> pyr	Aconitate	Pyruvate	A complex multistep reaction that occurs at medium speed and is accelerated by ferrous sulfide. The reaction can be quenched by scavenging of hydroxyl as well as sulfate radicals.
aco -> ssa	Aconitate	Succinic semialdehyde	A medium speed reaction that is accelerated by ferrous sulfide and requires decarboxylation and hydration of the substrate in a complex multistep reaction. This reaction cannot be quenched with sulfate or hydroxyl radical scavengers and presumably follows a radical independent mechanism.
aco -> suc	Aconitate	Succinate	A slow reaction which presumable complex multistep path that is facilitated by peroxydisulfate and is indifferent towards the presence and absence of ferrous sulfide. This reaction can also be facilitated to a minor extend using hydrogen peroxide, but is efficiently quenched with a sulfate radical scavenger.
akg -> mal	α-Keto glutarate	Malate	A slow interconversion that is observable in the peroxydisulfate conditions only. The overall reaction path includes a decarboxylation and a reduction reaction. This reaction can also be facilitated to a minor extend using hydrogen peroxide, but is efficiently quenched with a sulfate radical scavenger.

akg -> pyr	α-Keto glutarate	Pyruvate	A potential complex multistep reaction that is occurring at low rates and is slowed by the presence of ferrous sulfide, presumable due to the activation of competing reactions with α-ketoglutarate as substrate.
akg -> suc	α-Keto glutarate	Succinate	A fast decarboxylation reaction that is accelerated by ferrous sulfide. Efficiently quenched with sulfate radical scavengers. This reaction can also be facilitated by hydrogen peroxide, however at lower rates, as well as Fe(II).
cit -> pyr	Citrate	Pyruvate	Presumably ferrous sulfide accelerated reaction that is following a complex multistep reaction path. Likely to be independent of other pyruvate forming reactions described here as for example from isocitrate and α-ketoglutarate. In contrast to these, the citrate to pyruvate interconversion is not quenched by hydroxyl and sulfate radical scavengers.
cit -> ssa	Citrate	Succinic semialdehyde	Potentially result of a complex multistep rearrangement reaction that is accelerated by the presence of ferrous sulfide
cit -> suc	Citrate	Succinate	A slow multistep reaction that is different to the isocitrate to succinate reaction as it is not activated by ferrous sulfide. Furthermore this reaction can be partially also driven by hydrogen peroxide. However, scavenger experiments show a clearly stronger quenching of the reaction when sulfate radicals are targeted.
fum -> pyr	Fumarate	Pyruvate	Represents a complex multistep reaction that occurs at medium speed ad is accelerated by ferrous sulfide. The reaction can be quenched by scavenging of hydroxyl as well as sulfate radicals and is active at about ten-fold lower rates with hydrogen peroxide as radical donor.
fum -> suc	Fumarate	Succinate	A slow hydration reaction that is observed with peroxydisulfate, but not in combination with ferrous sulfide. This reaction can also be facilitated with hydrogen peroxide, however at lower rates. The reaction can be quenched by both, scavenging of hydroxyl and sulfate radicals.
ict -> aco	Isocitrate	Aconitate	An elimination / dehydratation reaction that is facilitated by peroxydisulfate and is slightly slower in combination with ferrous sulfide, presumably because of the activation of a series of other competing ferrous sulfide accelerated reactions. The reaction can be almost completely quenched by both, scavenging of hydroxyl as well as sulfate radicals.
ict -> akg	Isocitrate	α-Keto glutarate	A fast reaction involving the decarboxylation and oxidation of the isocitrate substrate. This reaction is accelerated by ferrous sulfide and can be efficiently quenched by sulfate radical scavengers. This interconversion is also efficiently catalyzed by Fe(II).
ict -> mal	Isocitrate	Malate	A fast reaction that possibly is the result of a complex multistep reaction and/or a more molecular complex rearrangement. In contrast to other malate forming reactions, which are facilitated by peroxydisulfate alone, strongly dependent on the presence of ferrous sulfide. Could represent an alternative isocitrate product that is generated by a separate reaction path than succinate, succinic semialdehyde and α-ketoglutarate.
ict -> pyr	Isocitrate	Pyruvate	Represents a potential complex multistep reaction that is occurring at medium rates and is accelerated by the presence of ferrous sulfide.

ict -> ssa	Isocitrate	Succinic semialdehyde	Possible routes for the generation of succinic semialdehyde are either the direct formation as a result of two decarboxylation of isocitrate at the positions C2 and C3, or the reduction of previously formed succinate. As the second reaction alone occurs slowly and ferrous sulfide independent (see below), the here observed fast and ferrous sulfide accelerated reaction is likely not to follow the latter path.
ict -> suc	Isocitrate	Succinate	A fast, presumable multistep reaction via α-ketoglutarate involving two decarboxylations and an oxidation. α-ketoglutarate is observed to be quickly formed from isocitrate. Interconversion rates measured for the α-ketoglutarate to succinate reaction are slightly faster and are in agreement with α-ketoglutarate representing a potential intermediate. The interconversion is dependent on sulfate radicals and is being accelerated by ferrous sulfide.
mal -> pyr	Malate	Pyruvate	Fast multistep reaction that is accelerated by ferrous sulfide and quenched by both, hydroxyl and sulfate radical scavengers. The reaction path involves a decarboxylation reaction in the proximity of a beta-hydroxyl group together with oxidation of this secondary alcohol to form a ketone.
mal -> suc	Malate	Succinate	A slow reaction only occurring in the absence of ferrous sulfide that could involve a dehydratisation of the 2-hydroxy moiety to alkene followed by hydration. A potential fumarate intermediate is not observed, however the fumarate to succinate reaction is considerably faster than starting from malate. Reaction is strongly driven by sulfate radicals, but also occurs at low rates with hydroxyl radical donors.
ssa -> pyr	Succinic semialdehyde	Pyruvate	Slow, presumable complex multistep reaction that is found at accelerated rates in the absence of ferrous sulfide, potentially because of the reduced rates of the alternative reaction forming succinate.
ssa -> suc	Succinic semialdehyde	Succinate	A fast dehydrogenase-like oxidation reaction requiring peroxydisulfate, presumably as oxidizing agent that is being clearly accelerated in the presence of ferrous sulfide.
suc -> pyr	Succinate	Pyruvate	Presumable complex multistep reaction that occurs at medium rates and is quenchable to approx. 50% with a sulfate radical scavenger and observable only in the presence of peroxydisulfate alone.
suc -> ssa	Succinate	Succinic Semialdehyde	Slow reduction reaction that is requiring a sulfate radical and is not substantially influenced by the presence or absence of ferrous sulfide.

UHPLC Gradient Supplementary Table 7 (Injection volume: 2 µl, autosampler temperature: 4°C, used for reaction characterisation)

Step	Time (min)	Flow (ml/min)	Solvent (%)
1	0	0.5	1
2	4.5	0.5	1
3	9.5	0.4	70
4	10	0.5	95
5	10.5	0.5	100
6	11.5	0.5	100
7	12	0.5	95
8	13	0.4	1
9	13.5	0.5	1
10	16	0.5	1

UHPLC Gradient Supplementary Table 8 (Injection volume: 2 µl, autosampler temperature: 4°C, used for testing the impact of individual metal ions):

Step	Time (min)	Flow (ml/min)	Solvent (%)
1	0	0.5	1
2	5	0.4	50
3	5.5	0.5	95
4	6	0.5	100
5	6.5	0.5	100
6	7	0.5	95
7	7.5	0.4	1
8	8.5	0.5	1

UHPLC Gradient Supplementary Table 9 (Injection volume: 1.5 µl, autosampler temperature: 40°C, column temperature 20°C, used for quantifying the reaction of oxaloacetate to pyruvate):

Step	Time (min)	Flow (ml/min)	Solvent (%)
1	0	0.5	10
2	3	0.5	60
3	3.3	0.5	100
4	4.3	0.5	100
5	4.5	0.5	10
6	5	0.5	10

UHPLC Gradient Supplementary Table 10 (Injection volume: 1.5 µl, autosampler temperature: 4°C, overlapped injection time 4.15 min, used for screening iron/sulfur environments):

Step	Time (min)	Flow (ml/min)	Solvent (%)
1	0	0.5	5
2	3.2	0.5	60
3	3.5	0.5	100
4	3.7	0.5	100
5	3.9	0.5	5
6	4.4	0.5	5

UHPLC Gradient Supplementary Table 11 (Injection volume: 2.5 µl, used for detailed elaboration of peroxydisulfate/ferrous sulfide impact on TCA metabolites)

Step	Time (min)	Flow (ml/min)	Solvent (%)
1	0	0.5	2
2	5,5	0.5	60
3	6	0.5	100
4	7	0.5	100
5	7.2	0.5	2
6	8	0.5	2

Supplementary Table 12: MS/MS parameters

Basic	
Instrument	Triple quadrupole mass spectrometer (Agilent 6460)
Software for data analysis	QQQ Quantitative Analysis
Scan type	Multiple Reaction Monitoring (MRM)
Ion source	XESI
Ion Mode	ESI + Agilent Jet Stream
Source parameters	
Gas temperature	300°C
Gas flow	8 L/min
Nebulizer	50 psi (nitrogen)
Sheath gas temperature	300°C
Sheath gas flow	11 L/min
Negative voltage	3000 V
Neg. Nozzle voltage	500 V

Positive voltage	3500 V
Pos. Nozzle voltage	500 V

Supplementary Table 13. MRM transitions and parameters

Compound	Parent ion mass	Product ion mass	Frag-mentor voltage [V]	Collision energy [V]	Retention time – short method [min]	Retention time - long method [min]	Polarity
Citrate	191	111	70	9	2.09	3.12	Negative
Cis-aconitate	173	129	56	5	2.23	3.26	Negative
		85.1	56	5	2.23	3.26	Negative
		41.1	56	13	2.23	3.26	Negative
α-ketoglutarate	145	101.1	56	5	1.97	2.79	Negative
		57.1	56	5	1.97	2.79	Negative
Malate	133.1	115.1	74	5	1.84	2.55	Negative
		71.1	74	9	1.84	2.55	Negative
Oxaloacetate	131	87	56	5	2.18	1.54	Negative
Succinate	117	73	52	5	1.59	2.13	Negative
Fumarate	115	71	44	0	2.11	2.97	Negative
Succinic semialdehyde	101.1	57.2	45	5	2.14	1.10	Negative
Pyruvate	87	43	55	3	1.31	1.46	Negative

Supplementary Figure 1

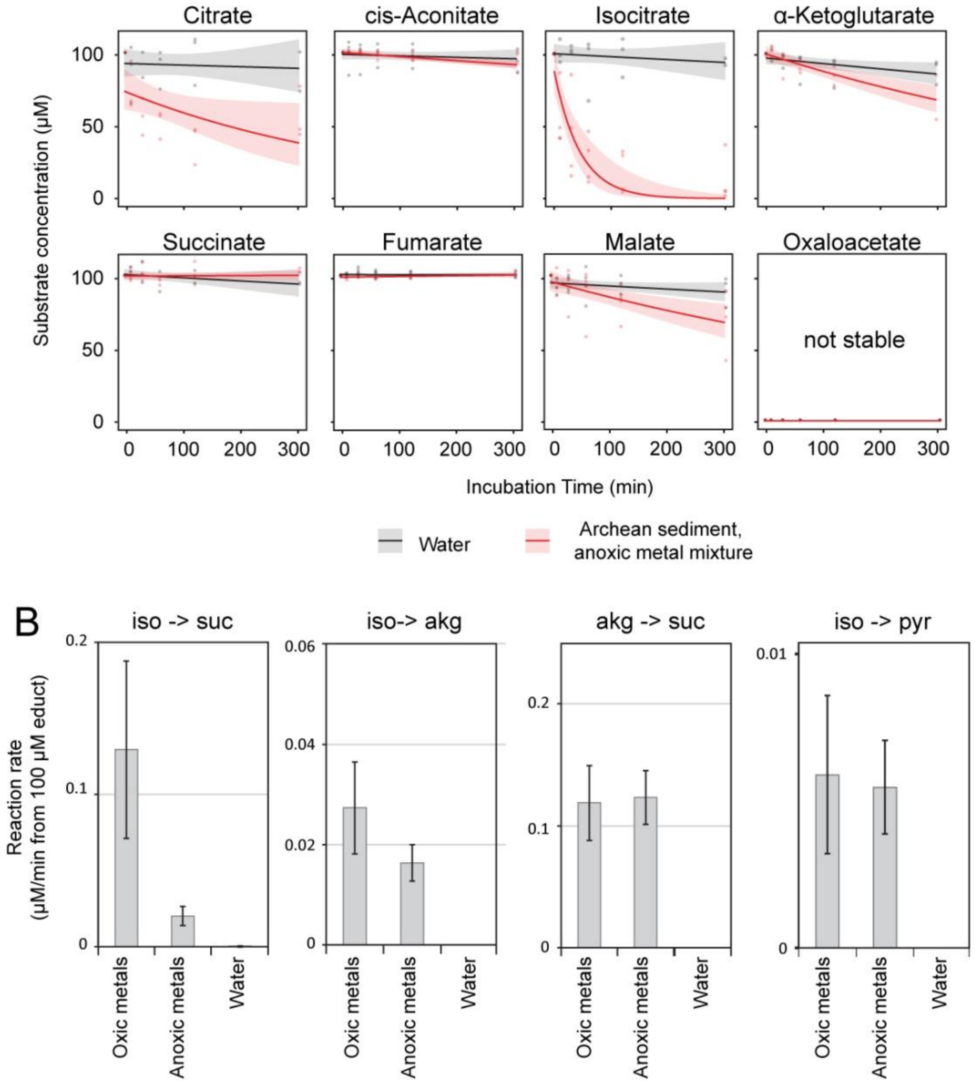

Supplementary Figure 1: **Absolute reaction rates and substrate stabilities in Archean sediment metal induced reactivity**: A) Stabilities of different TCA metabolites when incubated in presence and absence of metal mixture representative of Archean oceanic sediments at 70°C in triplicated time series for up to 5 hrs. Using liquid chromatography - selective reaction monitoring analytics the stabilities of substrate metabolites were measured. In pure water (black lines and circles) most TCA metabolites exhibit high stability, whereas an Fe(II) rich environment (red lines and circles) increased reactivity of citrate, isocitrate, alpha-ketoglutarate and malate to form other TCA metabolites. Oxaloacetate was an exception as it was rapidly converted into pyruvate in the water control (see Fig. S2 for details). Measured metabolite concentrations are represented by coloured circles. A local polynomial regression fitting model was fitted to the data. The fitting models are represented with lines and standard errors are indicated by coloured areas. B) Simultaneously, the formation of specific products was monitored by mass spectrometric analysis. The reactions isocitrate->succinate, isocitrate->α-ketoglutarate, α-ketoglutarate->succinate and isocitrate->pyruvate were observed in presence of an Archean sediment metal mixture under low-oxygen as well as normoxic conditions, whereas in a parallel water control a comparable TCA specific reactivity was not detectable.

Supplementary Figure 2

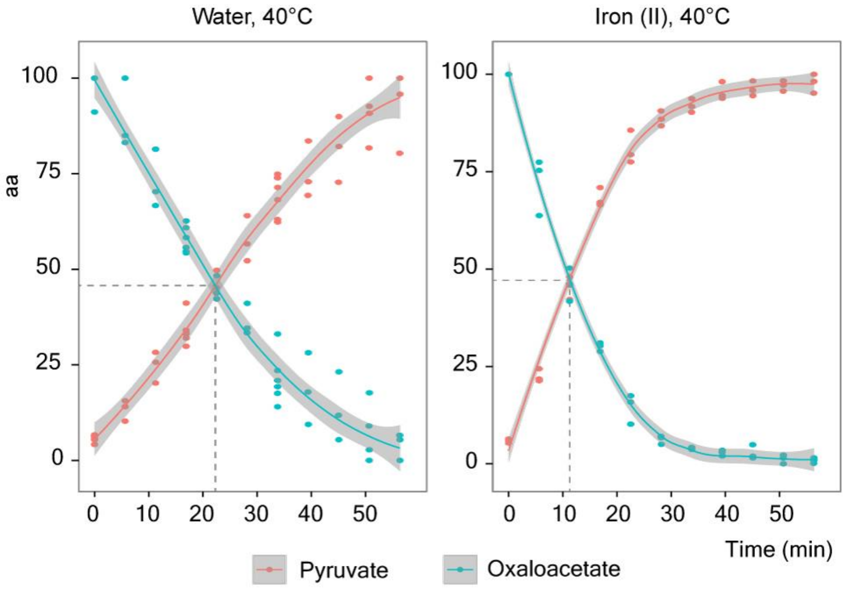

Supplementary Figure 2: **Non-enzymatic conversion of oxaloacetate into pyruvate.** Experiments performed at 70°C showed that the non-enzymatic reaction oxaloacetate->pyruvate was occurring in water and in Archean sedimentary conditions, but was too fast to be reliably quantified in the set-up used for following the other reactions. Hence we designed a separate series of experiments to analyse its reactivity at reduced temperature. Oxaloacetate was dissolved in water in the presence (right panel) and absence (left panel) of iron(II) chloride under normoxic conditions. The solution was transferred in a HPLC vial and incubated directly in the autosampler of the chromatographic system (Agilent 1290) at 40°C. Rapid injections of the solution every 5 minutes and immediate mass spectrometric quantification of the formed metabolites with a modified LC-SRM method were programmed. These results demonstrate that the interconversion of oxaloacetate -> pyruvate is accelerated by in the presence of Fe(II).

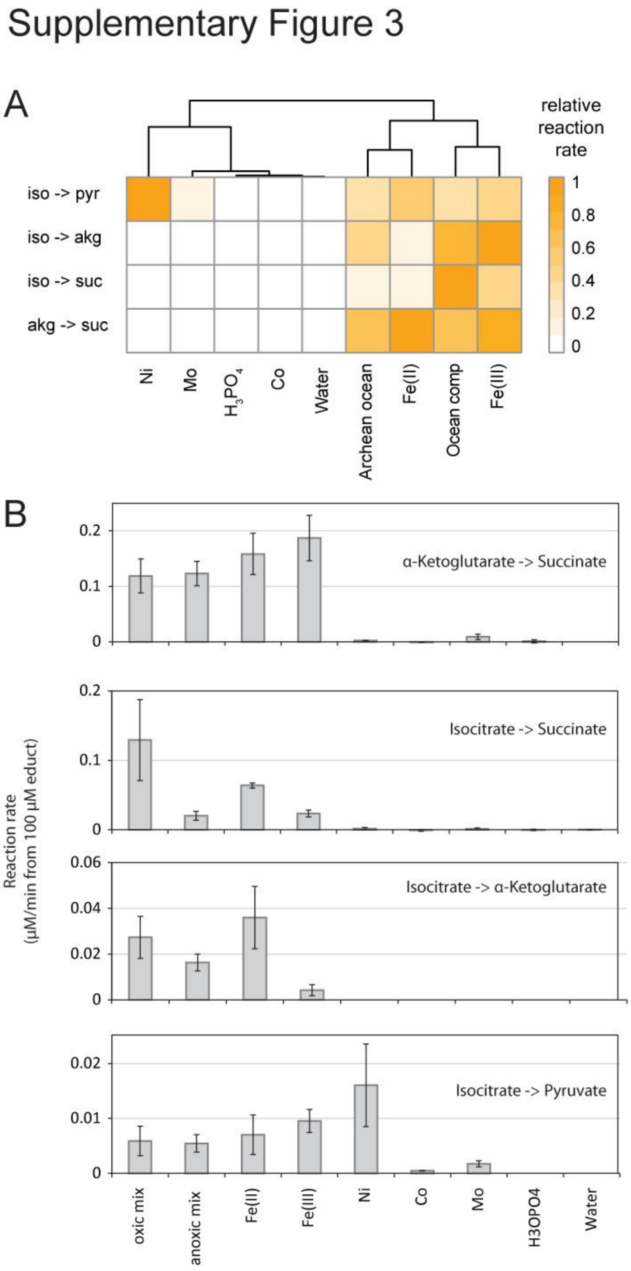

Supplementary Figure 3: **Metal dependency of non-enzymatic TCA-like reactions**: Individual metal constituents of the Archean sediment metal mixture were tested for their capacity to facilitate the observed TCA specific reactivity (see methods and Fig. S1). Additionally, the same experiment was conducted also for the complete metal mixture under normoxic and low-oxygen conditions. Product formation was followed in a time series up to 5h and quantified by LC-SRM. Reaction rates were determined by fitting of time dependent product accumulation data. A) Heatmap representation of rates normalized to the respective highest rate observed for each reaction. B) Absolute rates quantified for the same conditions. Fe(II)/Fe(III) were identified as main drivers of the observed non-enzymatic reactivity (Supplemental Fig individual metals)

Supplementary Figure 4

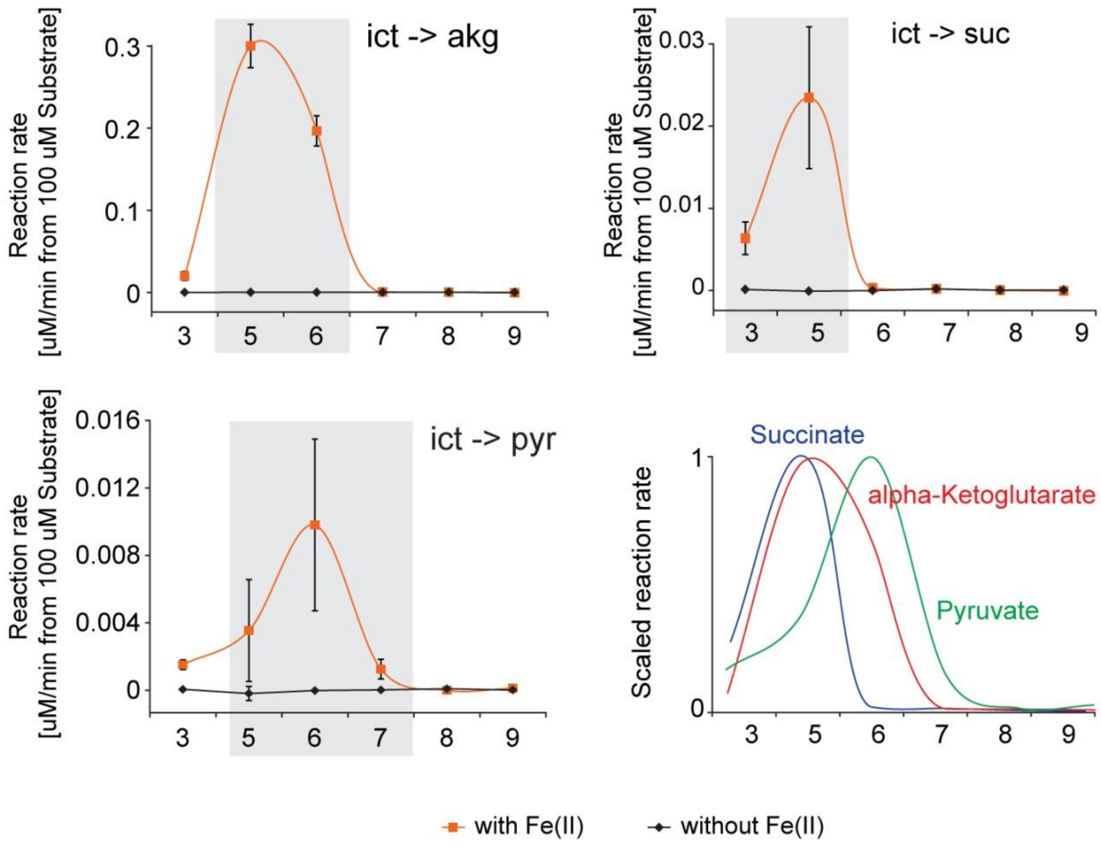

Supplementary Figure 4: **pH dependency of iron catalysed non-enzymatic interconversions with isocitrate as substrate**. 100 µM isocitrate were incubated at 70°C in the presence of 200 µM ferrous iron (orange) and water (black) in a time series of up to 300 min. A) pH dependent formation rates of α-ketoglutarate. B) pH dependent formation rates of succinate. C) pH dependent formation rates of pyruvate. D) pH profiles depicted in A-C were normalized to maximum values of 1 to allow a direct comparison. Reactivity could be observed in acidic conditions at pH 3-6, whereas in basic pH no non-enzymatic reactivity was observed. Overlay of individual pH dependency shows the different maxima of succinate and pyruvate formation (pH 5 and pH 6 respectively).

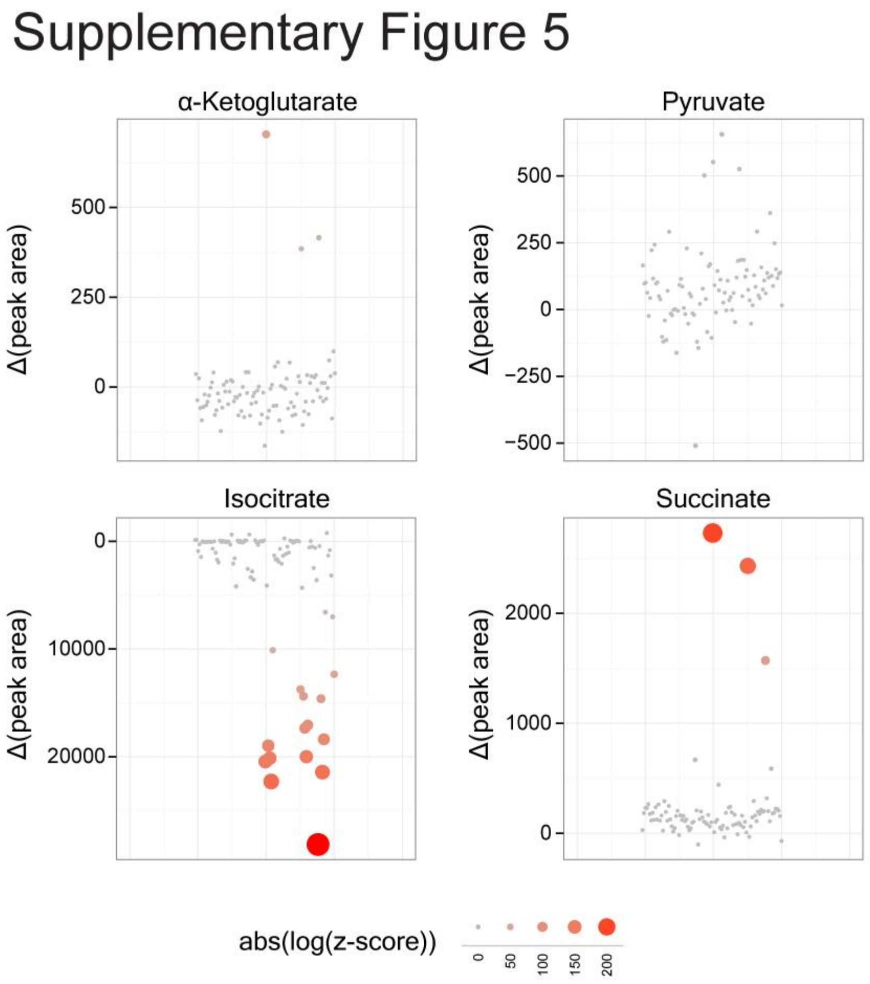

Supplementary Figure 5: **Exemplary representation of the distribution of Δ(peak area) values used for the subsequent determination of z-scores in the iron/sulfur screening illustrate for isocitrate as substrate**. Δ(peak area) values were calculated by subtracting LC-SRM measured metabolite responses for t=300 min from the t=0 min responses. In most cases these values were below or close to the signal/noise level and yielded a distribution around a Δ(peak area) of 0. In some cases however the formation of alpha-ketoglutarate, pyruvate and succinate as well as the consumption of isocitrate was observed, generating deviating Δ(peak area) values (depicted as circles). On basis of the resultant distribution, for each Δ(peak area) we calculated z-scores and p-values (see methods section). Absolute logarithmic z-score values are indicated by circle-size and colour saturation in each individual graph.

Supplementary Figure 6

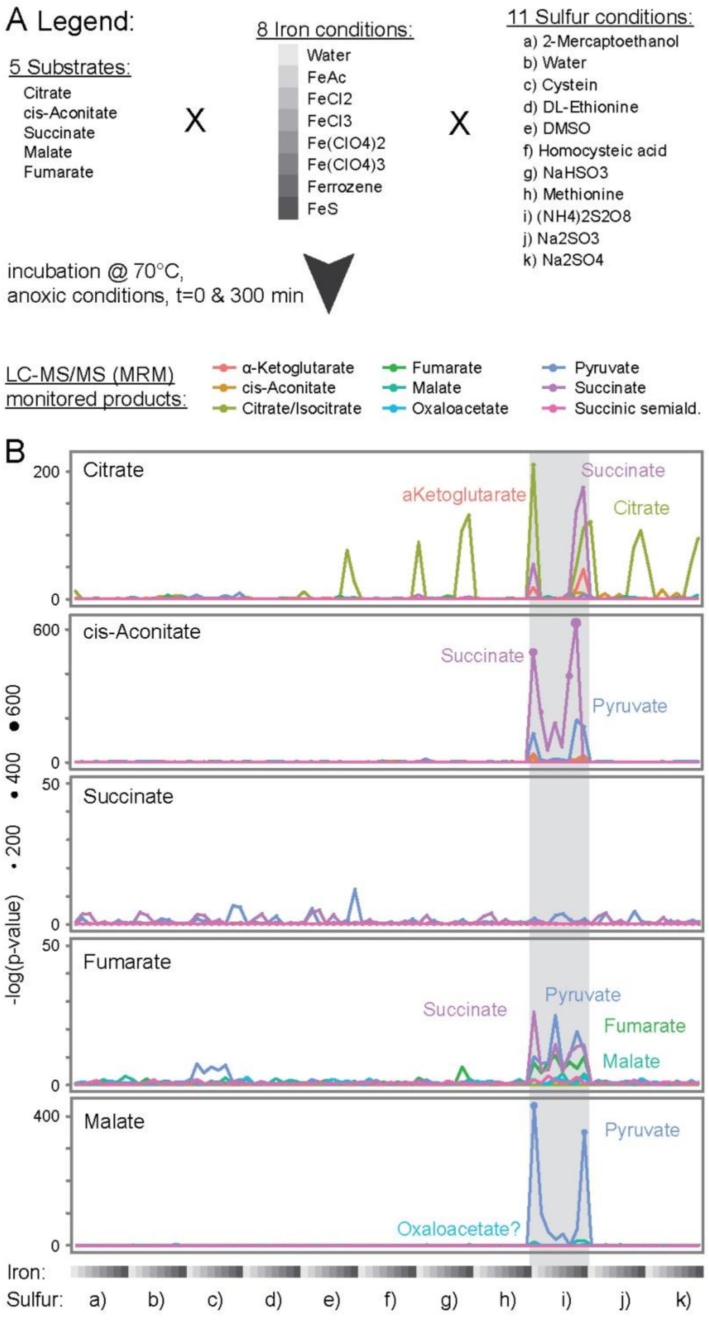

Supplementary Figure 6: **Graphical illustration of the iron/sulfur screening setup and illustration of complete results**. A) Five different substrates were incubated with combinations of 8 iron and 11 sulfur sources (both including a water control) for 0 and 300 min at 70°C in an artificial nitrogen atmosphere. Samples were subjected to LC-SRM analysis for quantification of specific products. Significance of product formation and substrate consumption was calculated as detailed in the methods section and Fig. S5. B) For each of the five substrates all 792 p-values obtained from the screening analysis are plotted against the 88 different conditions. Values are colour coded according to the measured metabolite product; circle size and position on the y-axis indicate the respective absolute logarithmic p-value. The peroxydisulfate containing conditions (indicated by the grey area) are characterized by a frequent and significant formation of specific products, especially when combined with ferrous sulfide.

Supplementary Figure 7

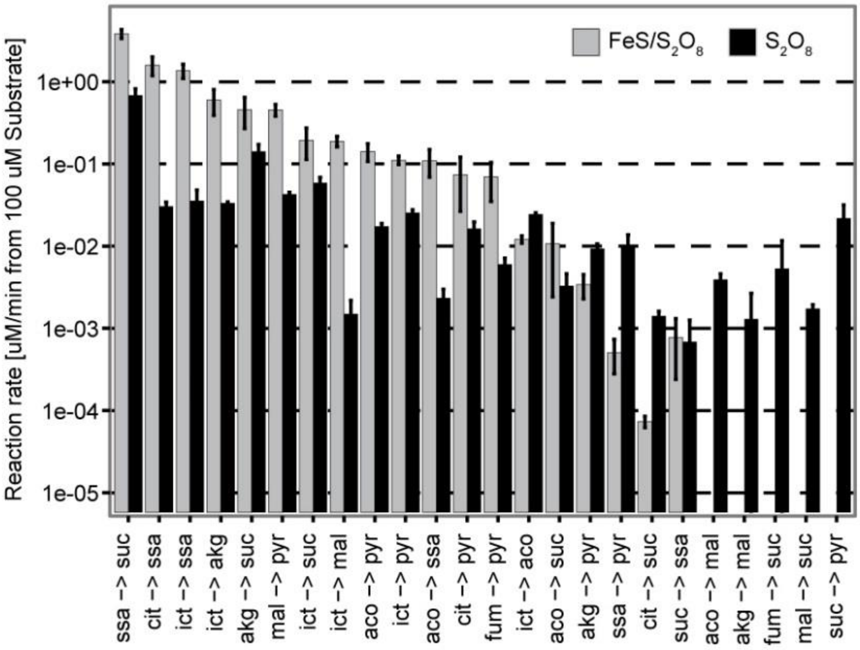

Supplementary Figure 7: **Absolute reaction rates of peroxydisulfate and ferrous sufide facilitated non-enzymatic TC-likeA reactions**. Reaction rates for non-enzymatic TCA reactivity in the presence of peroxydisulfate/ferrous sulfide (depicted network graph in Fig. 2D and heatmap in Fig. 3A), illustrated as bar chart. The rates are given in µM/min from 100 µM of the respective substrate and are shown as means ± SD, n=3. Please note the logarithmic scale of the y-axis.